FILE (2)

FINAL REPORT

ONR grant no: N00014-89-J-1476

Title of grant: Typhoon Prediction (Recurvature - 1990 Experiment)

Duration of grant: 11/01/88 - 04/30/92

Summary of work completed:

Recurvature Dynamics

A recent review paper, to appear in the journal *Advances in Atmospheric Sciences*, summarizes the work completed under this grant. A copy of this review is enclosed as an appendix to the report.

The approach we have followed is to first make a very high resolution model forecast of a recurving typhoon. Given a good forecast on the medium range with a comprehensive physical-dynamical model we next proceeded to evaluate residue-free budgets of vorticity and divergence following the model's output history. The residue-free budgets follow the model equations and thus carry a lot of useful information on the recurvature dynamics. Specifically, we have evaluated the residue-free budgets of vorticity and divergence for a 6 day period, Krishnamurti et al. (1992a). The salient aspects of the recurvature dynamics were as follows:

1. *Vorticity Budget*

We have examined the residue free budget based on the model forecasts over the four sectors of the typhoon following the track (see fig. 1). The sector averaged time history of vorticity budget for the forecasts for days 0, 1, 2, 3, 4 and 5 are of interest.

All of the terms of the vorticity equation were evaluated at all vertical levels and vertically averaged over the different sectors of the storm. Here we shall illustrate two of the important terms of the vorticity equation i.e. the advection of absolute vorticity ($-\vec{V} \cdot \nabla(\zeta+f)$) and the divergence term ($-(\zeta+f)\nabla \cdot \vec{V}$). The interesting results are for the forward and the right sectors and only those are illustrated in fig. (2a,b) respectively. The open vertical bars show the forward vertically averaged vorticity advection while the shaded vertical bars show the divergence term. In the forward sector, the vorticity advection is increasingly negative during the first 3 days of forecast, thereafter it becomes positive. The divergence term is positive throughout the history of the forecast over this sector. During the commensement of recurvature on days 2 and 3 of forecasts, the magnitude of the divergence term is roughly 30 to 50% of the magnitude of the horizontal advection term. That is by no means a negligible contribution. On day 5 of forecast, the divergence term is dominant over the front sector. The results for the right sector, shown in fig. (2b), show a nearly opposite time history for these two terms. Initially in the first three days, the vorticity advection is predominantly positive and as the recurvature is completed the vorticity advection becomes largely negative. The divergence term of the vorticity equation contributes to a generation of vorticity in the initial two days, thereafter changes sign and becomes very weak. During the early recurvature stage the divergence term is quite substantial. In Table (1) we show all of the terms of the vorticity equation for the right sector (vertically integrated through the model depth) for day 3 of forecast. The total tendency term is around 27×10^{-10} sec^{-2} for the right sector. Largely that is explained by horizontal advection 33×10^{-10} sec^{-2} and divergence term -6×10^{-10} sec^{-2}. The vertical advection and the twisting term nearly compensate. The remaining terms add up to a small total.

It should be emphasized that this is a single case study on the recurvature dynamics. More case studies need to be carefully examined. Overall, we note that the right sector encounters a strong positive vorticity tendency during the first 72 hours and that arises from positive vorticity advection and also from the divergence term of the vorticity equation. During this period, the front sector shows a negative contribution from the vorticity advection.

These are important factors that inhibit (or slow down) the due northwestward motion and contribute to the recurvature. The divergence term has a substantial contribution to the overall vorticity tendency of the storm motion.

Fig (3) is a schematic diagram of the typhoon outflow near the tropopause level. The cyclonic outflow turns into an anticyclonic outflow at the outer radii. At the transition radius where the cyclonic outflow changes to anticyclonic outflow nearly all of the outflow is a divergent flow.

2. *Advection of Divergence and the Divergence Square Contribution*

The advection of divergence and the divergence square terms for the forward sector in the outflow layer are shown in fig. (4). The time history of the evolution of these terms in the forward sector (averaged within a 5° latitude circle), are extremely interesting. Although these two terms compensate each other in the divergence equation, the difference between the two terms is roughly 20% of their mean value during the recurvature stage of the storm. This is very clear in fig. (4) where we examine the results for days 2, 3 and 4 when the storm was encountering its strong recurvature. The advection of divergence by the divergent part of the wind is positive and about 20% larger than the $-D^2$ term (which is negative, shown as $+D^2$ in this illustration to facilitate visual comparison of the two terms).

What about the $V\psi \cdot \nabla D$ term? The advection of divergence by the rotational part of the wind vanishes in the outflow layer where the inner cyclonic outflow changes to an outer anticyclonic outflow. This is true of most storms. Fig. (5a,b) illustrates the flow field and the stream function at 200 mb. This is actual flow chart for the storm and corresponds to the schematic presented in fig. (3). Along the outflow stream where the rotational part of the flow vanishes (and changes from cyclonic to anticyclonic) the entire flow field is divergent. This occurs within the five degree latitude radius of the predicted storm at 200 mb. The values of $V\psi \cdot \nabla D$ were in general, much smaller than those of $V\chi \cdot \nabla D$ and D^2 in the outflowing air over the forward sector. Within the forward sector, the advection by the rotational part is directed more towards the tangential direction, whereas the advection by the divergent part of the wind is more along the radial direction. Table (1) illustrates all of the terms of the divergence budget for the front sector at 200 mbs. for day 3 of the forecast when the storm was experiencing recurvature. The advection of divergence by the divergent part of the wind is indeed the largest term during the recurvature. The vertical advection and the twisting like terms are of opposite sign. The advection of divergence by the rotational part is roughly 1/3 of the magnitude of the advection of divergence by the divergent part of the wind. The results of the residue free budgets clearly show that the divergence term in the vorticity equation is quite large near the center of the storm in its inner rain area. Here the vertical motion (fig. 6) shows a gradual evolution of asymmetry with respect to the central position of the the recurving storm. An east-northeastward location of the strong upward motion center contributes to strong divergence in the right and front sectors during recurvature. That contributes to stronger values of the divergence term in the vorticity equation and of the advection of divergence by the divergent part of the wind in the divergence equation.

This robust residue free budget is extremely revealing on the recurvature aspect of this storm since the predicted track, intensity and structure were quite reasonably predicted by the model at the resolution T170.

Proposed Work

The Navy has expressed a considerable interest on the problem of storm motion. We have two excellent models, one a regional high resolution (see Table 2 and fig. 7 which show the successful forecasts of the recent Bangladesh storm) and multilevel very high resolution global model. We wish to continue exploration of residue free budgets in those cases where excellent forecasts on storm motion have been possible. We also plan to explore causes of failures where we have encountered difficulties. The TCM 90 data sets will form our best test beds for these studies. We will carefully address the validity of the TCM 90 and possibly also the TCM 92 hypothesis on storm motion. Two of my graduated students have received Navy fellowships, thus my contacts with the Monterey group have been considerably strengthened since I do go to Monterey quite frequently. I plan to keep in touch with the NRL group on numerical modelling and with NPGS on the storm motion dynamics. We feel strongly that we will be able to contribute further on these important typhoon motion and typhoon dynamic issues of importance to the Navy.

Table 1 Divergence and Vorticity Budgets.

Divergence Budget:

Forward Sector, Day 3.

Units $10^{-10}\ s^{-2}$

$-V_{\psi} \cdot \nabla D = -6.94$

$-V_{\chi} \cdot \nabla D = 21.39$

$-V \cdot \nabla D = 14.45$

$-D^2 = -15.45$

$-\dot{\sigma} \frac{\partial D}{\partial \sigma} = -15.95$

$\frac{-1}{a\cos\theta} \left[\frac{\partial \dot{\sigma}}{\partial \lambda} \frac{\partial u}{\partial \sigma} + \frac{\partial \cos\theta \dot{\sigma}}{\partial \theta} \frac{\partial v}{\partial \sigma} \right] = 16.68$

$\zeta f = 3.67$

$-\beta u = -2.14$

$2J(u, v) = -7.20$

$-\nabla \cdot (\alpha \nabla p + \nabla \phi) = -5.70$

$-K\nabla^4 D = 0.23$

$\nabla \cdot F = -0.06$

$\frac{\partial D}{\partial t} = -11.47$

Divergence = $4.83 \times 10^{-6}\ sec^{-1}$

Vorticity Budget:

Right Sector, Day 3.

Units $10^{-10}\ s^{-2}$

$-V_{\psi} \cdot \nabla \zeta = 23.598$

$-V_{\chi} \cdot \nabla \zeta = 9.066$

$-V \cdot \nabla \zeta = 32.663$

$-(\zeta + f)D = -5.914$

$-\beta v = -3.074$

$-\dot{\sigma} \frac{\partial \zeta}{\partial \sigma} = -6.381$

$\frac{-1}{a^2\cos\theta} \left[\frac{\partial \dot{\sigma}}{\partial \lambda} \frac{\partial \cos\theta v}{\partial \theta} - \frac{\partial \cos\theta \dot{\sigma}}{\partial \theta} \frac{\partial u}{\partial \lambda} \right] = 5.377$

$\frac{-1}{a^2\cos\theta} \left[\frac{\partial \alpha}{\partial \lambda} \frac{\partial p}{\partial \theta} - \frac{\partial \alpha}{\partial \theta} \frac{\partial p}{\partial \lambda} \right] = 4.602$

$-K\nabla^4 \zeta = 0.386$

$\hat{k} \cdot \nabla x \vec{F} = -0.827$

$\frac{\partial \zeta}{\partial t} = 26.832$

Relative Vorticity = $6.11 \times 10^{-6}\ sec^{-1}$

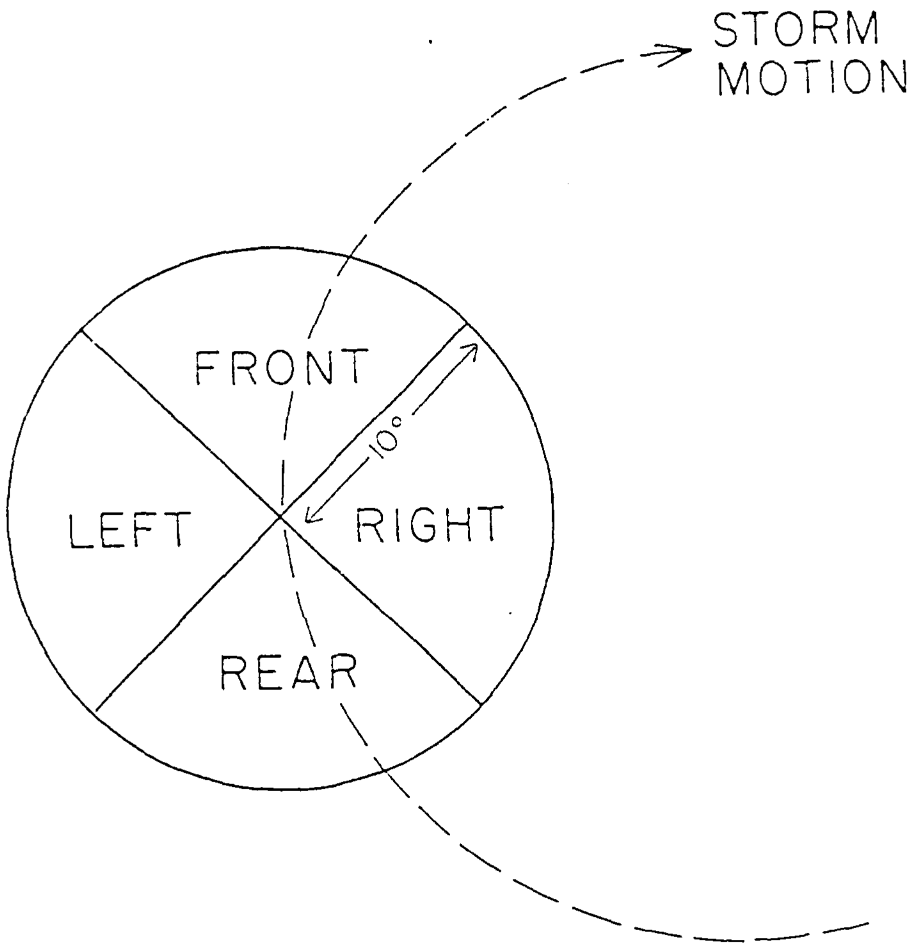
STORM
MOTION
FRONT
10°
LEFT
RIGHT
REAR

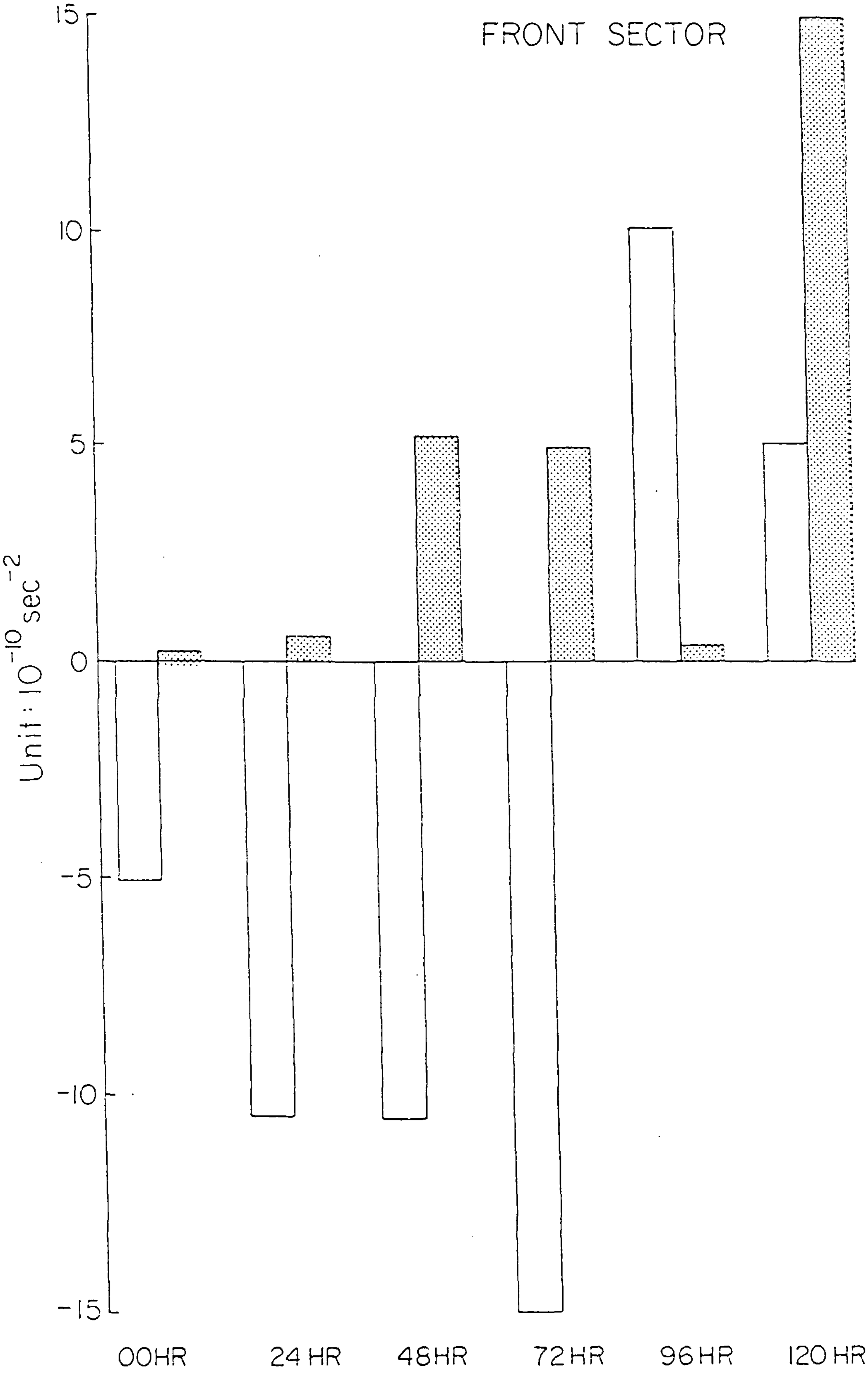
FRONT SECTOR
15
10
5
0
-5
-10
-15
Unit : 10^-10 sec^-2
00HR
24 HR
48HR
72HR
96HR
120 HR

2a

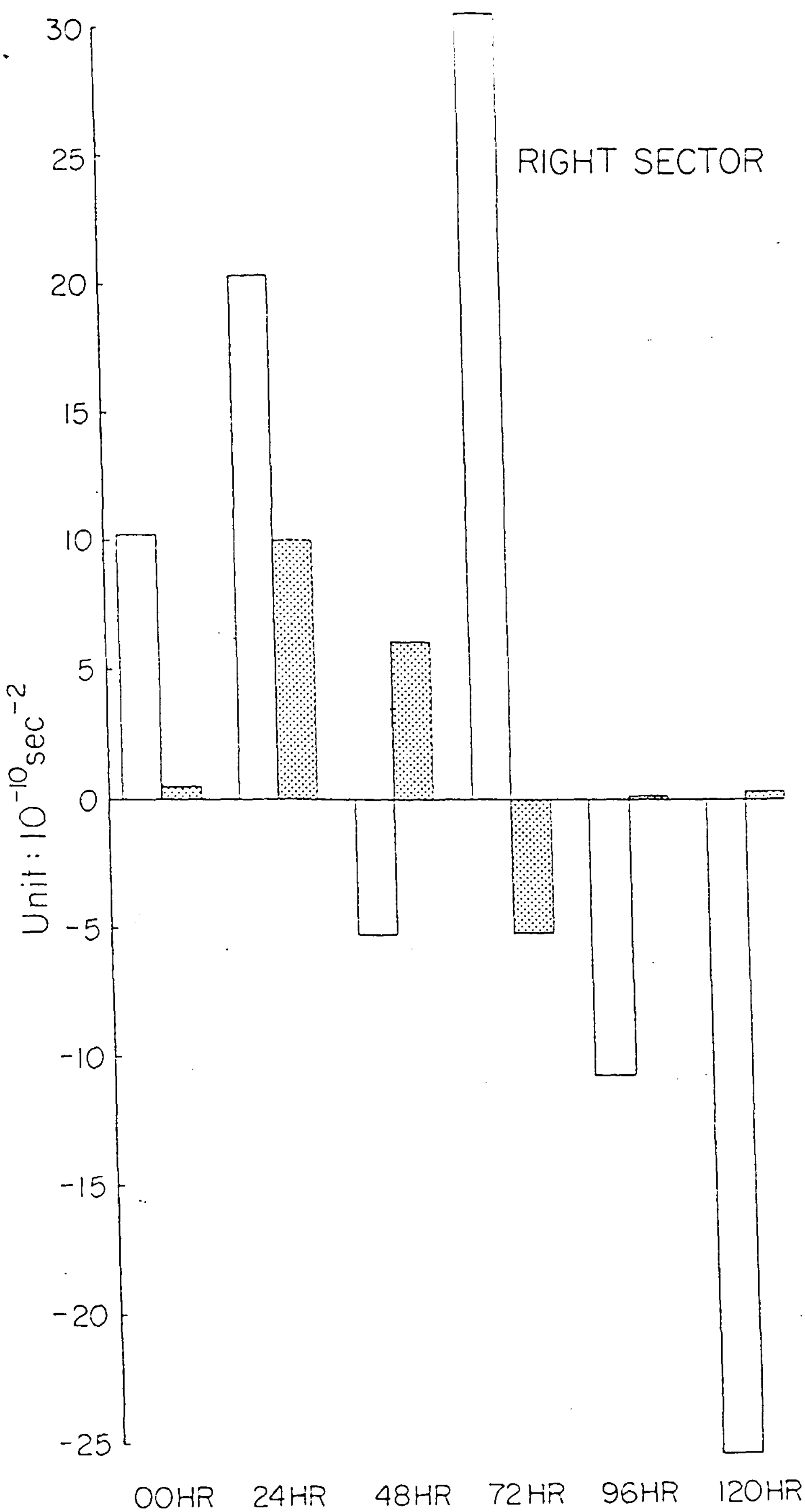
RIGHT SECTOR
Unit : $10^{-10}sec^{-2}$
30
25
20
15
10
5
0
-5
-10
-15
-20
-25
00HR
24HR
48HR
72HR
96HR
120HR

2b

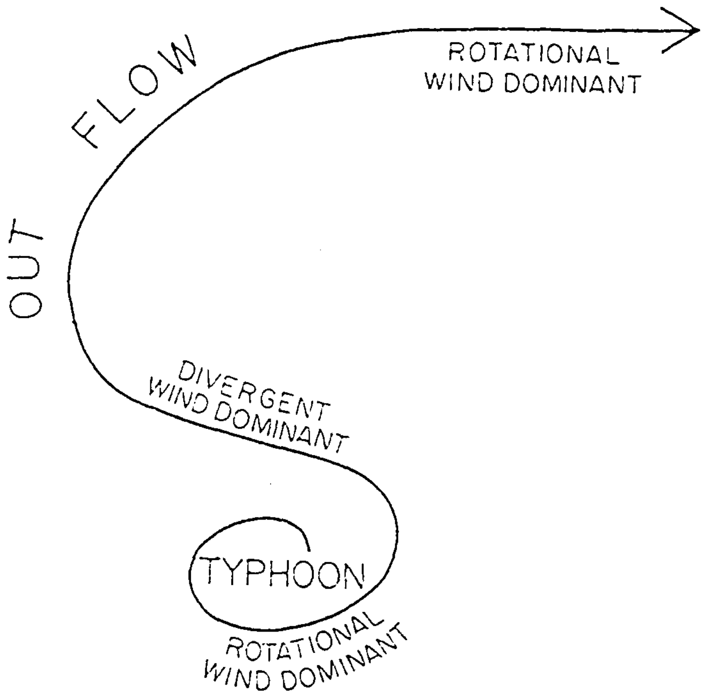
OUT FLOW
ROTATIONAL
WIND DOMINANT
DIVERGENT
WIND DOMINANT
TYPHOON
ROTATIONAL
WIND DOMINANT

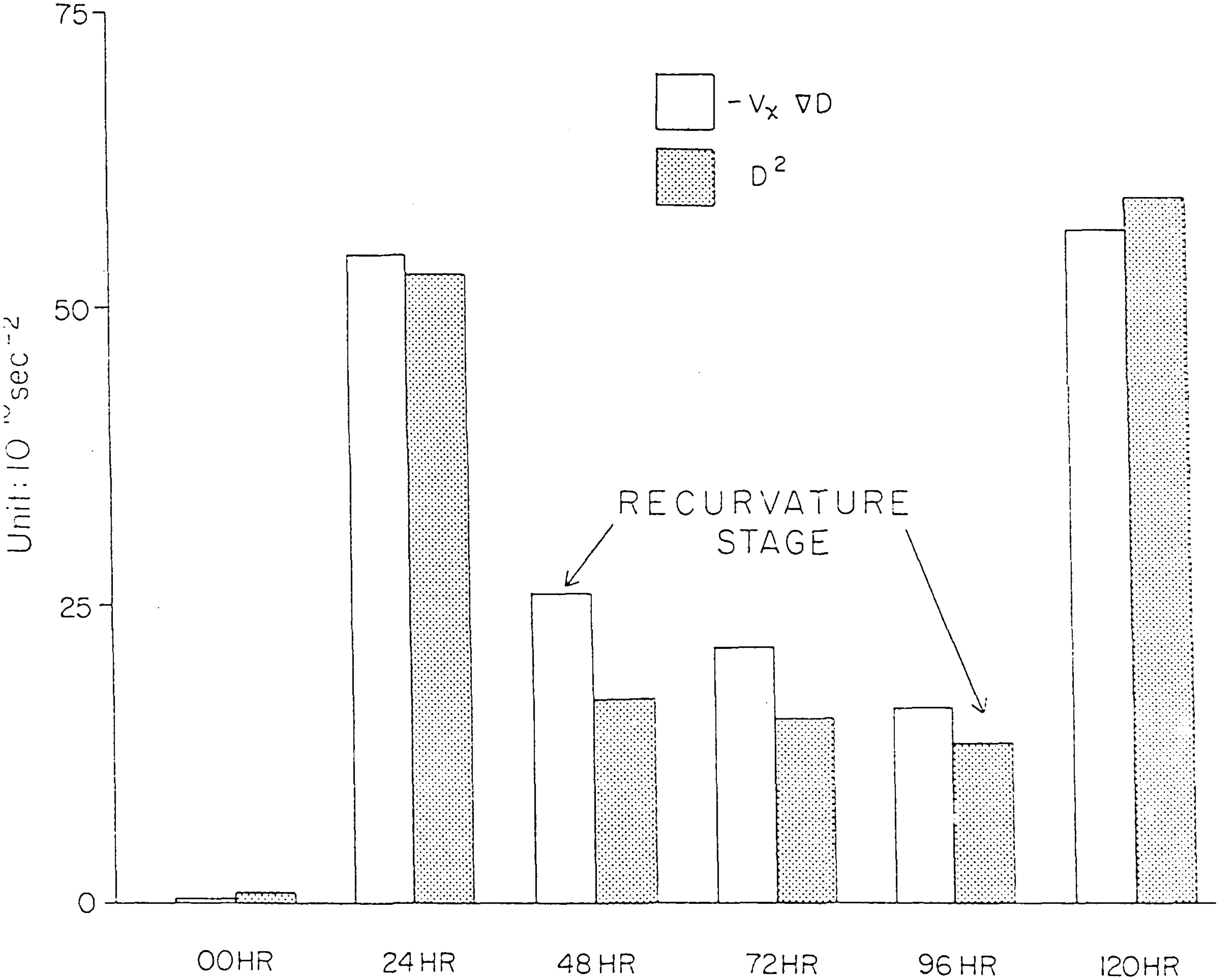

75
50
25
0
Unit: 10 ⁻¹⁰ sec ⁻²
$-V_x \nabla D$
D^2
RECURVATURE
STAGE
00HR
24HR
48HR
72HR
96HR
120HR

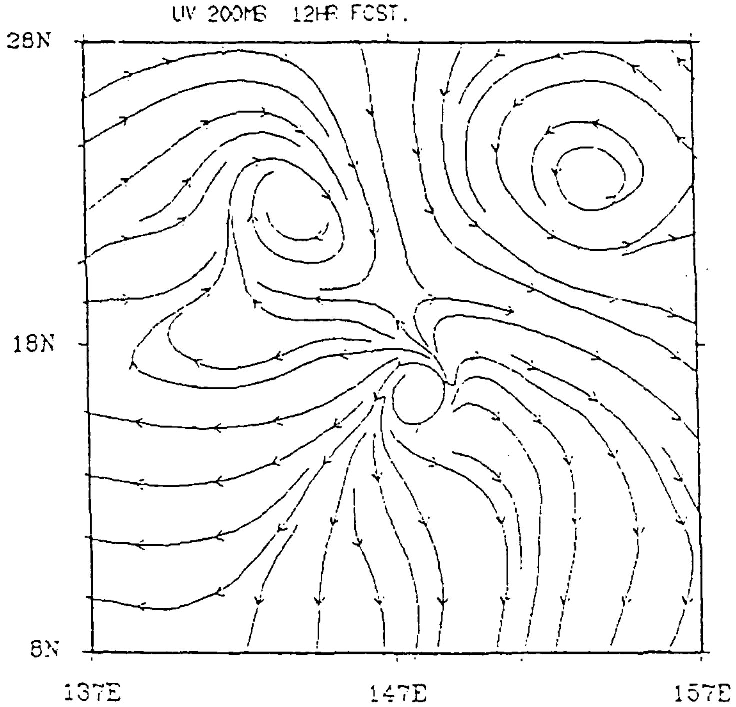
UV 200MB 12HR FCST.
28N
18N
8N
137E
147E
157E

a

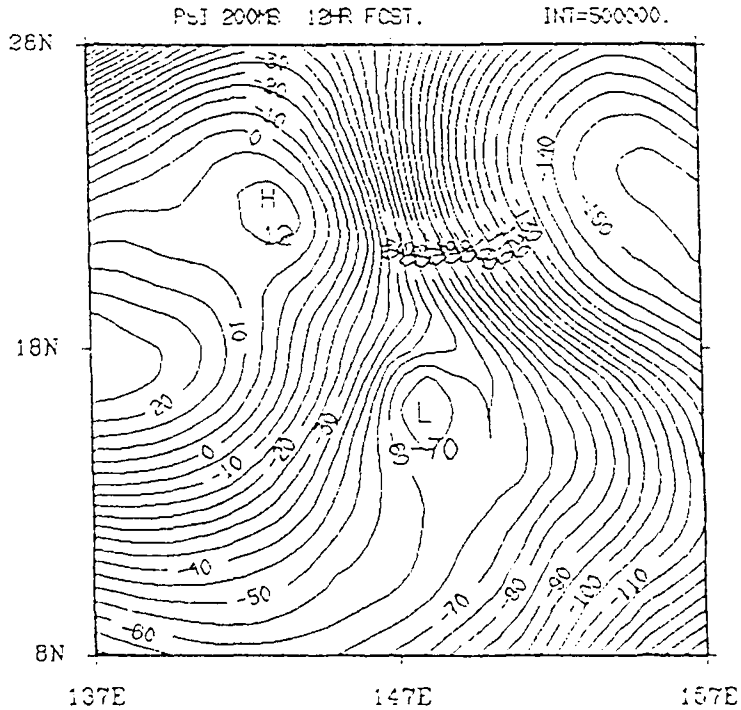
PSI 200MB 12HR FCST.
INT=500000.
28N
18N
8N
137E
147E
157E
H
L
-70
-60
-50
-40
-110

b

5a & b

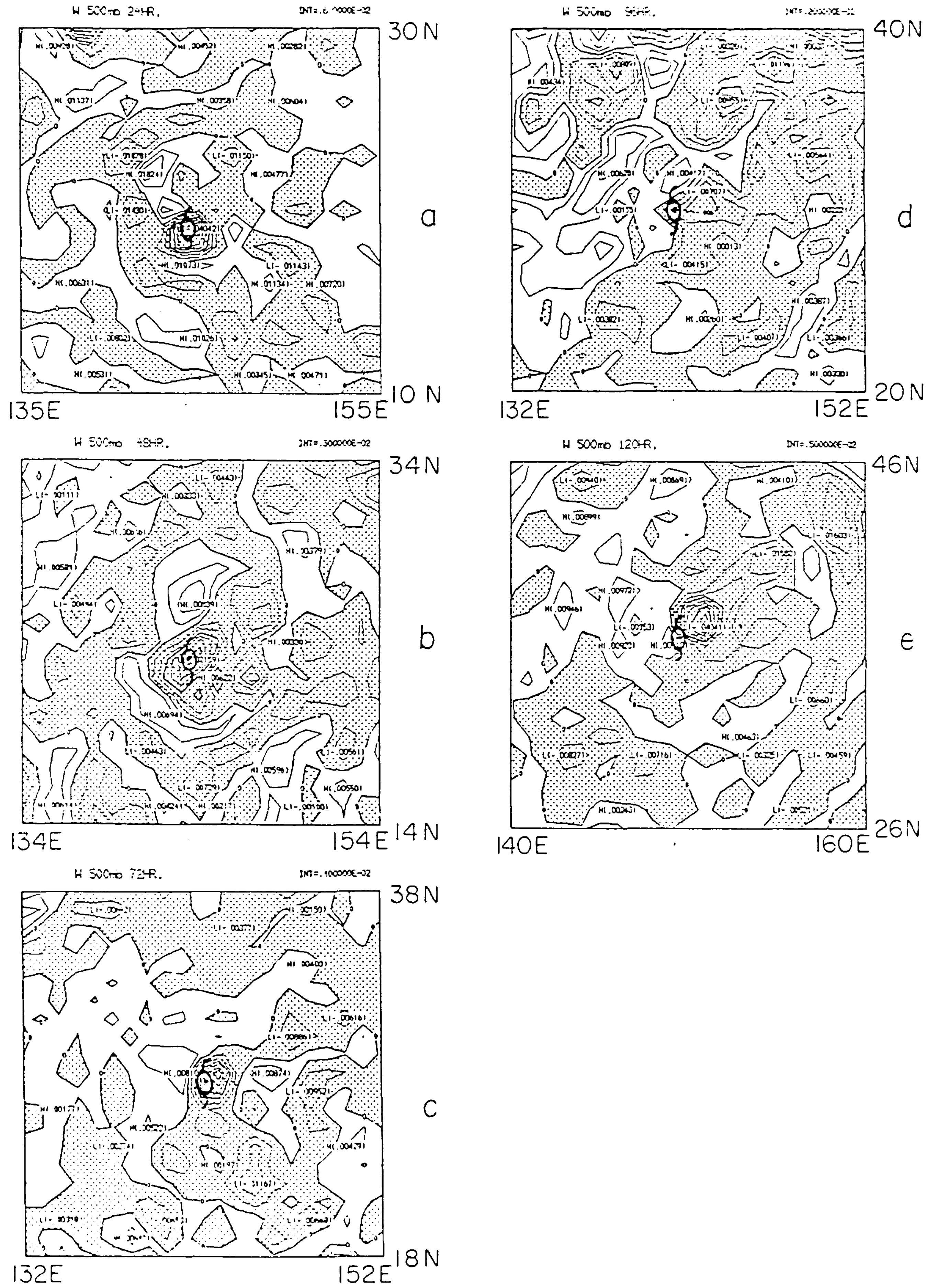

W 500mb 24HR.
30N
10 N
135E
155E
a
W 500mb 96HR.
40N
20N
132E
152E
d
W 500mb 48HR.
INT=.500000E-02
34N
14N
134E
154E
b
W 500mb 120HR.
INT=.500000E-02
46N
26N
140E
160E
e
W 500mb 72HR.
INT=.400000E-02
38N
18N
132E
152E
c

APPENDIX

ABSTRACT

A brief account of our studies on the hurricane forecast problem is presented here. This covers recent prediction results from the Florida State University (FSU) regional and global numerical weather prediction models. The regions covered are the Indian and the Pacific Oceans. The life cycle of the onset vortex (a hurricane) of the summer monsoon, typhoons over the western Pacific Ocean and tropical cyclones over the Bay of Bengal (Andhra Pradesh and the Bangladesh storms) are covered here. The essential elements in the storm formation are the strong horizontal shear in the cyclogenetic areas, a lack of vertical shear and warm sea surface temperatures. The storm motion has a steering component largely described by the advection of vorticity by a vertically averaged layer mean wind, the recurvature of a storm appears to invoke physical processes via the advection of divergence by the divergent part of the wind especially in the outflow layers of the storm. Very high resolution global models seem to be able to handle the motion and structure during the entire life of typhoons quite reasonably. The scope for better diagnosis of the storms life cycle appears very promising in view of the realistic simulation of the life cycle.

1. INTRODUCTION

With the great advances in global data assimilation, improvements in global modeling at very high resolution, incorporation of realistic physical parameterizations and initialization procedures (dynamical as well as physical) it has become possible to predict the entire life cycle of several hurricanes. This has required the use of the most advanced super computers. Major efforts have come from research laboratories, universities and operational weather services in Western Europe, United States and Japan. A brief review of these efforts is presented in the following sections.

2. DATA ASSIMILATION

A diverse system of global observations requires assimilation. They appear at different space-time location (asynoptic), they are based on measurements taken from space via satellites and from instruments launched daily from the earth's surface. This mixture of data is analyzed using what is called a multivariate optimal interpolation procedure within a four dimensional data assimilation. This invokes the use of the entire forecast model to perform assimilation in a continual basis as the data arrives. The elements of the data include the following:

a) Temperature, wind, pressure and humidity measurements from globally launched radiosondes and rawinsonde. This task is accomplished daily at around 00 and 12 UTC from roughly 900 weather stations.

b) Pilot balloon launches at the same, so called synoptic hours that are tracked by theodolites to provide wind measurements.

c) Marine data from ships of opportunity.

d) Flight level winds from commercial aircraft with inertial wind navigation.

e) Cloud tracked winds from the geostationary satellites.

f) Atmospheric soundings of temperature and humidity from operational polar orbiting satellites.

g) Marine data from oceanic buoys.

The analysis and assimilation are essential for the definition of the storm environment during its incipient stage.

3. THE HIGH RESOLUTION MODELS

The mesoscale horizontal resolution (≈ 50 kilometers) has been possible in the construction of regional and global models in recent years. It has also become evident that the simulations of hurricane structure and motion improve with resolution (Krishnamurti and Oosterhof, 1989). With the use of increased resolution it has been possible to simulate many details of the rainbands of the tropical cyclones (Dastoor and Krishnamurti, 1990). Overall in the global model, we have implemented resolution of the order of 170 waves (triangular truncation) and our regional model is currently running at a resolution of around 50 km. It is evident from these efforts that further improvement in horizontal resolution by about a factor of two may be needed to define the meso-β scale features of the tropical cyclones. In the vertical, roughly 15 layers resolve the troposphere and the stratosphere. We have also noted from these high resolution studies that the models continually assimilate the synoptic and sub-synoptic initial data sets to generate mesoscale shear flows in time. These appear to form at nearly the correct positions where strong organized convection evolves and contributes to the formation of hurricanes. The construction of four dimensional trajectories clearly shows that very high resolution models tap the information content from around the storm environment to describe cyclogenesis. The storms once formed move along reasonable tracks for periods of the order of a week. These are experimental forecasts of numerous storms that have been studied at the Florida State University (FSU). It has been noted that the track forecasts are quite sensitive to resolution and to the physics in the models. A coarse resolution model, by its very nature, has weak divergence, diabat' heating and rainfall. Storms forecasted by such models tend to deviate strongly from the observed tracks.

4. SENSITIVITY OF MODELS TO PHYSICAL PROCESSES

In the course of the storm forecast experimentations we have noted a large sensitivity to physical processes.

a) *Planetary Boundary Layer*

By far the largest impact comes from a proper representation of the surface layer physics. Robust fluxes of water vapor from the ocean are closely coupled to the tropical disturbances. In this area, one is dealing with supply of water vapor from remote evaporation (large scale) versus that from a more local environment of the storm (mesoscale). The latter requires a higher resolution model and an explicit treatment of the surface layer within the model computations, specifically we have designed a high vertical resolution for the surface layer to resolve the surface similarity fluxes explicitly. The lowest layer of the model is roughly 50 meters deep, which seems to be necessary for the modeling of the robust atmosphere - ocean coupling in the tropical cyclone environment. Lacking such a resolution, we have noted a general degradation of the forecasts and the absence of cyclogenesis. It should be noted that the hurricane scale cyclogenesis is not entirely a dynamical evolution. Wide spread rainfall precedes the storm formation within tropical depressions and easterly waves.

b) *Deep Cumulus Convection*

The parameterization of deep cumulus convection is a central issue in tropical numerical weather prediction. For a review of the various propositions for the inclusions of deep cumulus convection in large scale numerical prediction model a review paper by Molinari and Dudek (1991) is recommended. A number of schemes for the parameterization of cumulus convection exist. Of these we make use of a modified Kuo scheme. This makes use of available large scale moisture convergence to define deep convective cloud elements. The modified parameterization has been calibrated against data sets from field experiments where the large scale heating and moistening and the rainfall rates are optimized against observations via empirical statistical refinements. Such an ad hoc statistical correlation procedure is deemed necessary since the cloud space scale is of the order of a few km while the model resolution is much lower. The use of such a cumulus parameterization has proven to be extremely useful for the forecast of hurricanes. In typhoon prediction, rainfall totals of the order of 400 mm/day are not easily handled by many of the available cumulus parameterization schemes. With the proposed optimization of the Kuo scheme, it has been possible to account for these very high rainfall rates. It should be stated that improvements in the planetary boundary layer physics is a necessary prerequisite, i.e. to provide the large evaporation rates from the ocean and thus to account for these large rainfall rates from the cumulus convection algorithms. The planetary boundary layer physics and the cloud modeling are closely coupled.

c) *Radiative Transfer*

Processes such as diurnal change, maintenance of tropical (moist) conditional instability and effects of cloud - radiative interactions are also central issues for medium range forecasts. This requires detailed calculations of radiative transfer i.e. the fluxes and flux convergence of the short and long wave radiances. Sophisticated radiative transfer algorithims based an a band model take into account the heating and cooling rates from the major atmospheric constituents such as water vapor, carbon dioxide and ozone. The calculations include the effects of clouds which are estimated over different vertical layers of the atmosphere through a relative humidity criteria. An important role of shallow stratocumulus clouds that are abundant in the hurricane environment is to provide and maintain cloud top cooling near the 700 mb level which is roughly 3 km above the ocean. This cooling contributes to the maintenance of conditional instability of the hurricane environment. That energy is continually tapped by the inflowing of air into the inner rain area of the hurricane. This has been shown to be an important element in medium range forecasts of hurricanes (Krishnamurti et al., 1991a). Another factor that contributes to the maintenance of the conditional instability of the hurricane environment is the strong evaporation of air from the ocean. In that sense care needs to be exercised in the modeling of the surface layer physics and the radiative transfer algorithims. The success of forecasts crucially depend on the closely coupled physical algorithims that one puts together.

Other aspects of the radiative transfer include the calculation of surface energy balance-especially over the land areas. Here even factors such as soil moisture and ground wetness have an important role in the prediction of the landfall of hurricanes (Dastoor and Krishnamurti, 1990). These surface hydrological parameters require parameterizations which are functions of the surface albedo, surface humidity, past rainfall and ground elevation above sea level.

The landfall and subsequent motion of the storms (after landfall) does seem to be affected by the surface conditions such as dryness or wetness of land. The onset vortex of the monsoon over the Arabian sea coast is known to traverse towards the Arabian coast. Its inland penetration is almost totally inhibited by the dryness of land surface, these aspects of storm prediction have been successfully handled by our models that include sophisticated parameterizations of the land surface processes.

5. OROGRAPHY

The inclusion of steep orography in high resolution models is especially important for storms that traverse in their vicinity. Current modeling efforts include what is labelled "envelope orography", that is an enhanced orography which enables us to handle flow around the orographic barriers better. In its absence a significant part of the flows pass over the mountain chains leading to large track errors for the storm motion. An example was again the onset vortex whose motion, in the absence of steep Western Ghats of India led to an erroneous motion towards central India when in fact it was to move offshore along the west coast of India and eventually make landfall over the Oman Coast (Krishnamurti et al., 1984). The inclusion of envelope orography provided a successful forecast of the storm to almost a week.

6. INITIALIZATION

Because of inherent data errors the mass and the motion fields generally exhibit an imbalance. This imbalance leads to spurious wave motions that contaminate the initial stages of the forecast fields. To overcome this, the high frequency noise is generally removed by a procedure called the normal mode initialization. This is a standard procedure for dynamical initialization. In addition to that a physical initialization is considered desirable especially for the tropical latitudes (Krishnamurti et al., 1991(b)). Here one attempts to enhance the conventional data sets described in section 2 with the satellite based measures of rainfall rates. This procedure allows the model to basically accept these rain rates as an organic part of the prediction system at the initial time. This procedure improves the initial definition of the divergent wind and the diabatic heating i.e. consistent with the prescribed rain rates. The physical initialization is also designed to improve oceanic fluxes of water vapor and the overall distribution of clouds (i.e. consistent with satellite imagery). Given the general lack of data over the oceanic tropics this procedure augments the current observing system.

7. DIAGNOSTIC STUDIES OF FORECAST OUTPUT

Given a reasonable forecast on the medium range time scale from a multi level high resolution global model, it is possible to interrogate the history tapes of such forecasts. They provide an invaluable data source for the interpretation of storm forecasts. During the formative stage one can ask what the relative roles were for the various dynamical (such as shear flow instabilities) and physical processes. Likewise during the recurvature one can ask what were the salient physical processes. Our studies affirm that the relative role of strong horizontal wind shear, weak vertical wind shear, warm sea surface temperature and organized convection were some of the major processes during the storm formation in the Arabian sea. Further studies are needed to explore the formative mechanisms in other ocean basins. The computations for our diagnostic studies are carried within a residue free budget framework. These are carried out by precisely following the algorithms of the model during the model forecasts. The budget studies of vorticity and divergence are particularly revealing for the recurving storms. They show that the advection of vorticity by layer mean (i.e. vertically averaged) winds fails to account for the recurvature of forecast tracks. Further details such as the advection of divergence by the divergent part of the wind, especially in the upper troposphere outflow layer of the storms appears to play a crucial role in the recurvature problem. Almost simultaneously as the divergence is advected by the divergent wind in the outflow layer, low level convergent flow evolves in the planetary boundary layer via Dines compensation. This region becomes enriched in deep cumulus convection, thus contributing to a storm motion in the direction of this advection. This feature is most pronounced in the forward right quadrant of the storm motion. On the other hand the vorticity advection by the layer mean wind tends to be largest in the front and the left sector with respect of the storm motion. The storm appears to recurve along a resultant track which lies between those of the advection of the divergence and the advection of vorticity. The precise definition requires further detailed analysis of the residue free budgets. Since divergence is closely related to the heating and precipitation fields, recurvature is not entirely a dynamics problem, physical processes seem to be vital for its understanding.

8. RESULTS OF STORM FORECASTS

a) A non-recurving storm - Typhoon Hope of 1979 (Krishnamurti and Oosterhof, 1989)

Typhoon Hope formed over the Western Pacific on July 29, 1979, at around 17°N and 130°E. The observed (best fit) and the predicted tracks are illustrated in figure 1. Also shown in this illustration is the track at the coarse resolution T21. The latter shows a due westward motion of the storm. The track forecast based on a shallow water spectral model forecast, at a resolution of T170 is also shown in this illustration. The forecasts with the complete physics at the highest resolution T170 appear to be far superior to the other two forecasts on the medium range. We have noted that the track forecasts during the first two days are reasonably handled with dynamical models (at the resolution T21 the physical processes, especially convection is too weak). The robust rainfall history at T170 appears to be an important element for the improved track forecast. Figure 2 illustrates the predicted rainfall at the resolution T170, where the 24 hour rainfall amounts reached an amplitude of 453 mm/day between day 2 and 3 of the forecast. A high level of rainfall activity was predicted during the entire life cycle of this typhoon. The evolution of storm wind intensity at 850 mb for T170, as a function of radial distance from the storm center, is shown in figure 3. Also marked along the ordinate are the observed estimates of the strongest winds. On the whole, this was a rather successful forecast.

b) Typhoon Colleen of 1989, a recurving storm:

The approach we have followed is to first make a very high resolution model forecast of a recurving typhoon. Given a good forecast on the medium range with a comprehensive physical-dynamical model we next proceeded to evaluate residue-free budgets of vorticity and divergence following the model's output history. The residue-free budgets follow the model equations and thus carry a lot of useful information on the recurvature dynamics. Specifically, we have evaluated the residue-free budgets of vorticity and divergence for a 6 day period, Krishnamurti et al. (1992a). The salient aspects of the recurvature dynamics were as follows:

i) The middle tropospheric vertical motions are slightly off centered with respect to the storm center. This provides an interesting geometry for the divergence term in the vorticity equation. The divergence term of the vorticity equation contributes to a generation of vorticity on the east and front section of the storm during the recurvature. A major contributor to the slight asymmetry of the vertical motions is noted to arise from the advection of divergence from the divergent part of the wind. That is most pronounced in the outflow layer, i.e. near 200 mb. The outflowing air is cyclonic in the storms interior and anticyclonic in the storms exterior (beyond a 100 km radius). In the transition between the cyclonic and anticyclonic radii the outflow is almost entirely divergent. It is this region where the advection of divergence by the divergent part of the wind is dominant. Where the upper level divergence is advected lower layer convergence simultaneously evolves via Dines compensation and ensuing deep convection contributes to the enhancement of large scale vertical motions which are asymmetric to the storm center. Table 1 presents a sample of residue-free budget for the forward and the right sector for day 3 of the forecast. This table illustrates the importance of the advection of divergence by the divergent part of the wind and the divergence term of the vorticity equation.

c) *Formation of an Atlantic Hurricane: Frederic - 1979:*

A near perfect forecast on the formation of this storm made us inquire as to the mechanisms for the formation of Hurricane Frederic of 1979 over the Atlantic Ocean. The following two diagrams show the spectacular formation. Figure 5 illustrates the history of the prediction of 850 mb wind speed at 3 hourly intervals starting from hour 3 and ending at hour 72 of the forecast. Figure 6 illustrates the 3 hourly rainfall totals predicted by the model. Given these forecasts a detailed diagnosis of the storms energetics and angular momentum budgets were carried out. The storm forms out of an incipient African wave which amplifies by the barotropic process and eventually with the organization of surface friction the storm growth is attributed to the convective process. The increased growth of the easterly wave contributes to the steady expansion of the area of influence i.e. air is drawn into the heavy convective area from the outside. The angular momentum budget shows a growth of the hurricane scale arising from the convergence of flux of high angular momentum air from the outer radii that causes a rapid spin up of the storm on the mesoscale. The eventual wind speeds attained by the storm's circulation are a function of the frictional torques that are partly exerted by surface stresses and partly by the internal stresses contributed by up and down motions in rain areas along the inflowing air. The details of this study are presented in Krishnamurti et al. (1992b).

9. CONCLUDING REMARKS

Much progress has been made on very high resolution hurricane forecasting in recent years. The progress stems from availability of special data sets, advances in supercomputing and in the steady improvements in initializations and modelling strategies. Only a review of selected case studies are presented here. The operational experience is another story. For instance when we see the many daily forecasts made by the global weather centers on a single storm such as Hurricane Hugo of 1990 one notes a variety of skills in the track predictions. Some initial states apparently provide superior forecasts compared to others. This calls for research on ensemble forecasts and for the development of strategies for the definition of initial perturbations for the definition of ensembles. We expect this to be an area of future thrust. Further improvement in data analysis, initialization, model physics and diagnostics is expected in the coming years. The details of the inner storm area such as the eye wall circulations and rain bands were handled extremely by Dastoor and Krishnamurti (1990) with a very high resolution regional model. That resolution was around 45 km for the separation distance of the grid points in the horizontal. The same storm run with a global model at a resolution T106 (106 waves triangular truncation) fails to define the details of the eye wall or the rain bands). This model has an effective resolution of around 200 km. Thus it appears that for medium range prediction of hurricanes and typhoons we need resolutions of the order of T300 for the global model.

10. ACKNOWLEDGEMENTS

The research reported here was supported by NSF grant no. ATM-8812053 and LAWS grant no. NAG 8-761 AND LAWS contract no. NAS5-30932. Computations were performed

on the CRAY/YMP at NCAR.

REFERENCES

Dastoor, A.P. and T.N. Krishnamurti, 1990: The landfall and structure of a tropical cyclone: the sensitivity of model predictions to soil moisture parameterization. Boundary Layer Meteor., 55 345-380.

Krishnamurti, T.N., K. Ingles, S. Cocke, T. Kitade and R. Pasch, 1984: Details of low latitude medium range numerical weather prediction using a global spectral model. Part II: Effects of orography and physical initialization. J. Meteor. Soc. Japan, 62, 613-649.

Krishnamurti, T.N. and D.K. Oosterhof, 1989: Prediction of the life cycle of a super typhoon with a high resolution global model. Bull. Amer. Meteor. Soc. 70, 1218-1230.

Krishnamurti, T.N., K.S. Yap and D.K. Oosterhof, 1991(a): Sensitivity of Tropical Storm Forecast to Radiative Destabilization. Mon. Wea Rev., 119, 2176-2205.

Krishnamurti, T.N., J. Xue, H.S. Bedi, K. Ingles and D. Oosterhof, 1991(b): Physical initialization for numerical weather prediction over the tropics. Tellus, 43AB, 53-81.

Krishnamurti, T.N., H.S. Bedi, K.S. Yap, D. Oosterhof and G. Rohaly, 1992a: Recurvature dynamics of a typhoon. To be published in J. Meteor. Atmo. Phy.

Krishnamurti, T.N., V. Hardiker, J. Bevin, D. Oosterhof, 1992b: On the formation of hurricane Frederick of 1979. To be published in Tellus.

Molinari J. and M. Dudek 1992: Parameterization of convective precipitation in mesoscale numerical models: A critical review. To be published in Mon. Wea. Rev., 1992.

FIGURE CAPTIONS

Fig. 1 Barotropic (T170) and spectral (T170, T21) forecasts are compared with the best-fit tracks. Days of forecast are indicated on the side of the tracks.

Fig. 2 Predicted 24-hourly rainfall fields (T170) for day 1, 2, 3, 4, 5 and 6 for Typhoon Hope units are mm/day.

Fig. 3 Time history of the radial profile (along the direction of maximum wind) at 850 mb for days 0, 1, 2, 3, 4, 5 and 6 of the forecast. (T170).

Fig. 4 Observed (Guam best-fit) and the predicted tracks (multilevel spectral forecast at T170) for Typhoon Colleen. Day zero corresponds to October 3, 1989, 00 UTC. Labels along the track denote hours after initial time.

Fig. 5 Predicted 850 mb isotachs (multilevel spectral forecast at T170) for Hurricane Frederic at 3 hourly intervals. Hour zero corresponds to August 30, 1979, 00 UTC.

Fig. 6 Same as Figure 5 except for 3 hourly cumulative precipitation.

Table 1 Divergence and Vorticity Budgets.

Divergence Budget:

Forward Sector, Day 3.

Units 10^{-10} s^{-2}

$-V_{\psi} \cdot \nabla D = -6.94$

$-V_{\chi} \cdot \nabla D = 21.39$

$-V \cdot \nabla D = 14.45$

$-D^2 = -15.45$

$-\dot{\sigma} \frac{\partial D}{\partial \sigma} = -15.95$

$\frac{-1}{a\cos\theta} \left[\frac{\partial \dot{\sigma}}{\partial \lambda} \frac{\partial u}{\partial \sigma} + \frac{\partial \cos\theta \dot{\sigma}}{\partial \theta} \frac{\partial v}{\partial \sigma} \right] = 16.68$

$\zeta f = 3.67$

$-\beta u = -2.14$

$2J(u,v) = -7.20$

$-\nabla \cdot (\alpha \nabla p + \nabla \phi) = -5.70$

$-K\nabla^4 D = 0.23$

$\nabla \cdot F = -0.06$

$\frac{\partial D}{\partial t} = -11.47$

Divergence = 4.83 x 10^{-6} sec^{-1}

Vorticity Budget:

Right Sector, Day 3.

Units 10^{-10} s^{-2}

$-V_{\psi} \cdot \nabla \zeta = 23.598$

$-V_{\chi} \cdot \nabla \zeta = 9.066$

$-V \cdot \nabla \zeta = 32.663$

$-(\zeta + f)D = -5.914$

$-\beta v = -3.074$

$-\dot{\sigma} \frac{\partial \zeta}{\partial \sigma} = -6.381$

$\frac{-1}{a^2\cos\theta} \left[\frac{\partial \dot{\sigma}}{\partial \lambda} \frac{\partial \cos\theta v}{\partial \theta} - \frac{\partial \cos\theta \dot{\sigma}}{\partial \theta} \frac{\partial u}{\partial \lambda} \right] = 5.377$

$\frac{-1}{a^2\cos\theta} \left[\frac{\partial \alpha}{\partial \lambda} \frac{\partial p}{\partial \theta} - \frac{\partial \alpha}{\partial \theta} \frac{\partial p}{\partial \lambda} \right] = 4.602$

$-K\nabla^4 \zeta = 0.386$

$\hat{k} \cdot \nabla x \vec{F} = -0.827$

$\frac{\partial \zeta}{\partial t} = 26.832$

Relative Vorticity = 6.11 x 10^{-6} sec^{-1}

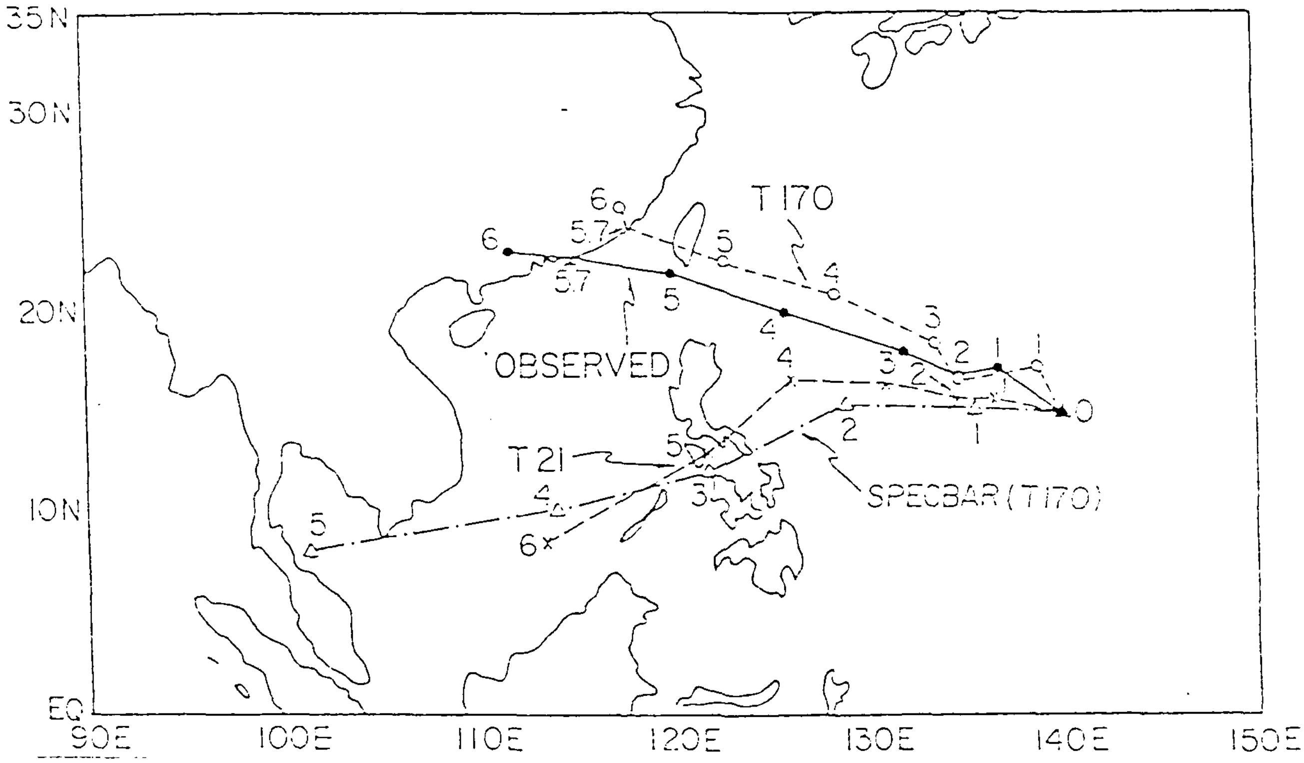
35N
30N
20N
10N
EQ
90E
100E
110E
120E
130E
140E
150E
T170
OBSERVED
T21
SPECBAR (T170)

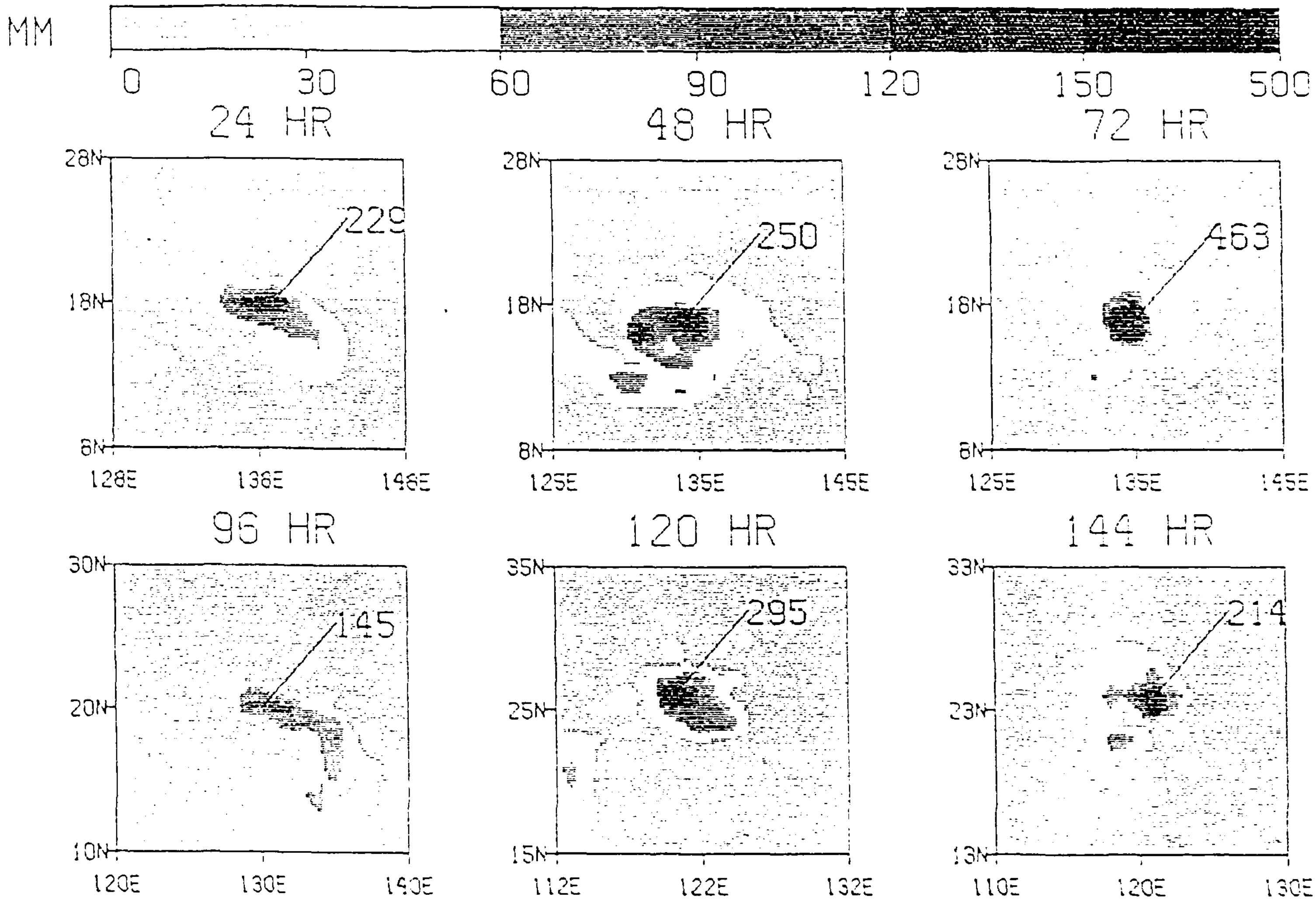

PREDICTED RAINFALL TYPHOON HOPE (1979)

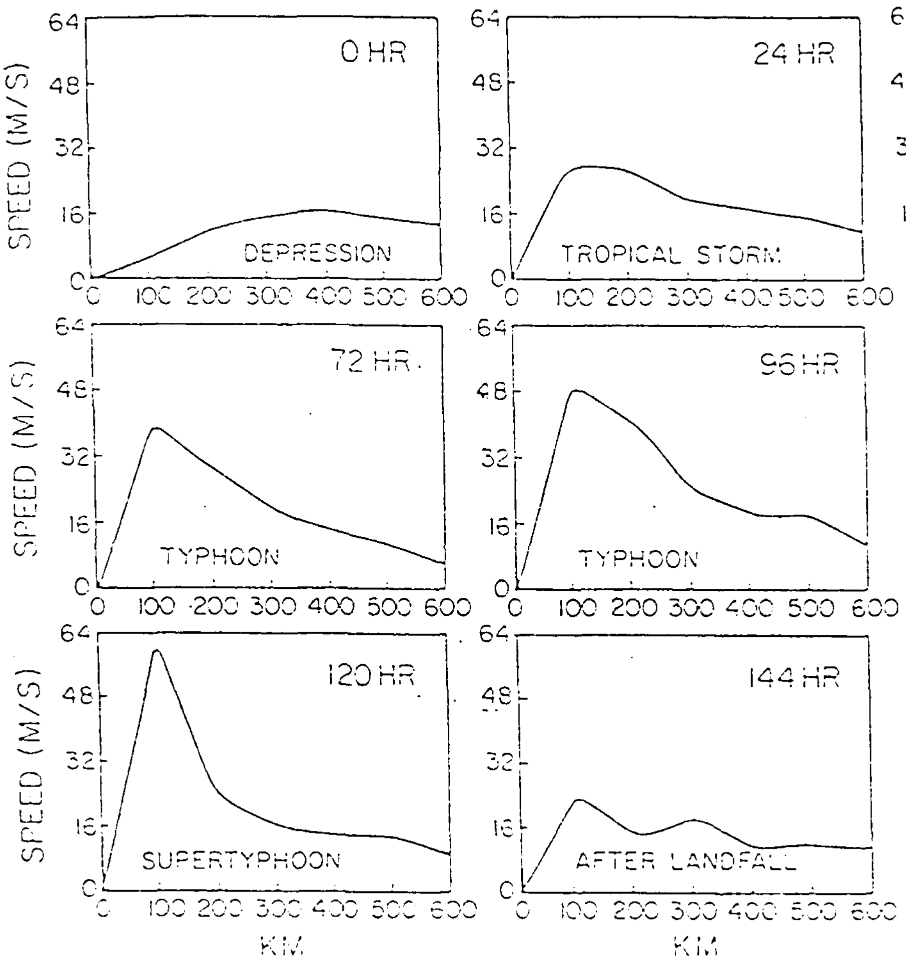

LIFE CYCLE OF
A SUPERTYPHOON
T 170

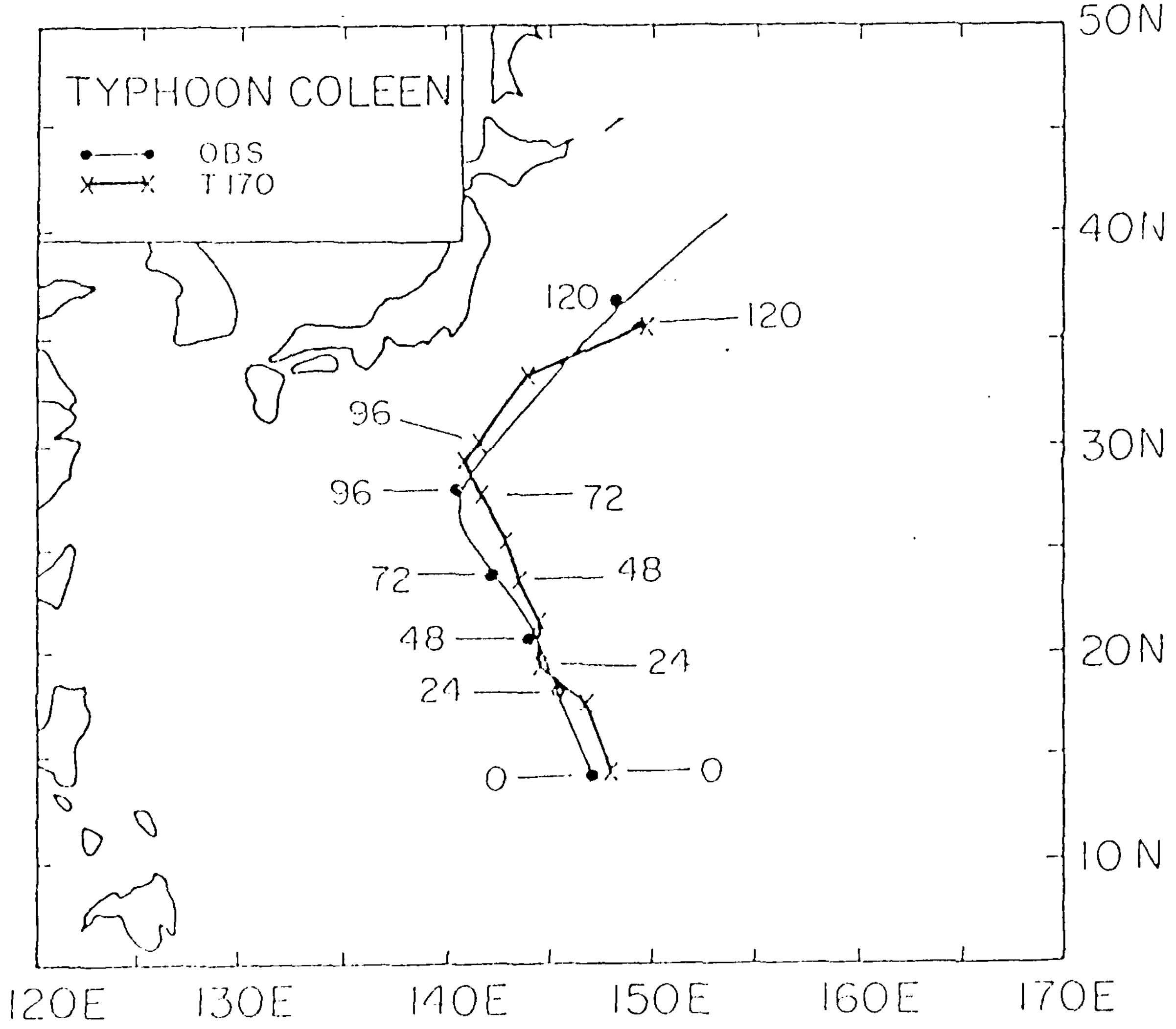
TYPHOON COLEEN
OBS
T 170
120
120
96
96
72
72
48
48
24
24
0
0
50N
40N
30N
20N
10N
120E
130E
140E
150E
160E
170E

FREDERIC T170 FCST WIND SPEED 850MB

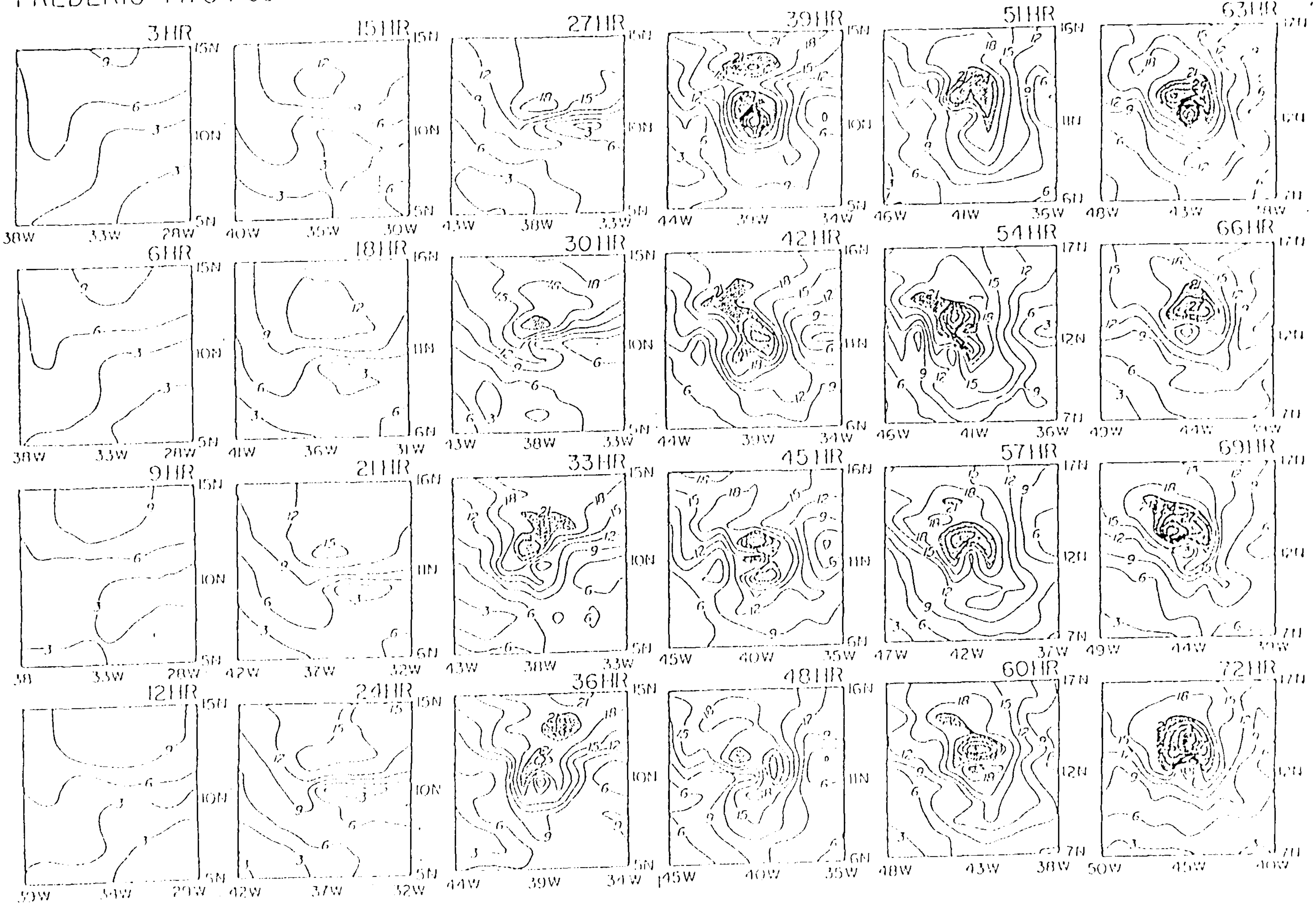

FREDERIC T170 FCST 3HR CUM PCP